Operational Reliability Evaluation of Distributed Multi-energy Systems Considering Optimal Control of Energy Storages

Sheng Wang
College of Electrical Engineering
Zhejiang University
Hangzhou, China
wangsheng_zju@zju.edu.cn

Yi Ding
College of Electrical Engineering
Zhejiang University
Hangzhou, China

Menglian Zheng
College of Energy Engineering
Zhejiang University
Hangzhou, China

Chengjin Ye
College of Electrical Engineering
Zhejiang University
Hangzhou, China

2021 IEEE/IAS Industrial and Commercial Power System Asia (I&CPS Asia) | 978-1-6654-3498-0/21/$31.00 ©2021 IEEE | DOI: 10.1109/ICPSAsia52756.2021.9621617

***Abstract*—Distributed multi-energy system (DMES) provides a flexible option to coordinate multiple energies, e.g., electricity, gas, heating, and cooling, to realize a more optimal operation. However, the tight interconnection of multiple energies may bring challenges to maintaining its reliability. The previous studies mainly focus on long-term reliability, which cannot reflect the time-varying reliability during the operation. This paper proposes an operational reliability evaluation approach for the DMES. Firstly, the operational reliability models of two typical types of components in the DMES are established. Then, an optimal control problem when the components fail is formulated. Moreover, the time-sequential Monte Carlo simulation technique is utilized to evaluate the operational reliability. Finally, a test case is used to validate the proposed reliability evaluation technique.**

Keywords—operational reliability, distributed multi-energy system, time-sequential Monte Carlo simulation

I. Introduction

Distributed multi-energy system (DMES) is emerging recently, as a means to coordinate multiple energies, such as electricity, gas, heating, and cooling, in local districts, such as campuses, buildings, etc. [1]. Typical energy-related devices in these districts include combined heat and power (CHP) plants, gas boilers (GB), electrical heat pumps (EHP), electrical energy storage (EES), etc. In Denmark, the electricity generation from local CHP has raised by 13% from 2015 to 2016, where natural gas takes 25.84% of the fuel consumption [2]. In China, the heat demand of nearly 9×10^9 m^2 area is supplied by centralized heating supply, 51% of which is met by CHP[3]. It is witnessed that by coordinating the operating condition of these devices, the operating cost or other indices of DMES can be optimized.

On the other hand, due to the tight links among those devices, the failure of one component will cause sequential effects on other components, and cause potential reliability issues. For example, the failure of CHP might lead to insufficient heat supply and further lead to the deration of the cooling production of absorption chillers (AB). Therefore, the reliability of DMES should be comprehensively studied considering the interdependency of multiple devices.

The research is supported by the National Key Research and Development Program of China under Grant 2017YFB0903400.

The reliability of DMES is studied in previous researches. The concept of energy hub (EH) is usually used to characterize the energy conversion relationships in the DMES [4]. The reliability model of EH was proposed based on the state space method in [5]. Considering the thermal dynamics in the buildings of the end-users, the reliability was further analyzed in [6] using the Monte Carlo method. Multi-parametric linear programming was used in [7] to improve the computation efficiency of the reliability evaluation. In [8], the DMES was further decoupled into the distribution network and end-user levels and evaluated the adequacy of multi-energy supplies. Considering the DMES with a large share of distributed renewable generations, multi-dimensional reliability indices were evaluated in [9] with both centralized and decentralized control strategies. The calculation of multi-energy flows was further decoupled in [10] to determine the optimal load shedding and used the impact-increment method to improve the computation efficiency. A smart agent-based method was also proposed in [11], and calculated the first-order reliability.

However, these studies mainly focus on steady-state reliability, where the probabilities of components in each state are regarded as a constant. This is applicable in the long-term, but not so accurate in the short term. In the short term, due to the time-varying load curve, and the scheduled maintenance and unit commitment, the reliability is supposed to be time-varying. On the other hand, due to the participation of multiple energy storages, the DMES can reschedule the energy utilization in the time horizon, and therefore can significantly improve the reliability during the operation. Therefore, the operational reliability of DMES is worth studying considering these two factors.

This paper develops an operational reliability evaluation technique for the DMES considering the optimal operation strategy with various energy storages. Firstly, the operational reliability models of the devices in the DMES are developed, using the Markov model to represent the time-varying state probability during the operation. Then, in each scenario with component failures, an optimal control method is formulated to minimize the electricity, heating, and cooling load curtailments, and the various energy storages are considered. Moreover, the time-sequential Monte Carlo simulation (TSMCS) method is used to evaluate the operational reliability. The proposed method is finally validated using a test case.

II. Structure of the Studied DMES

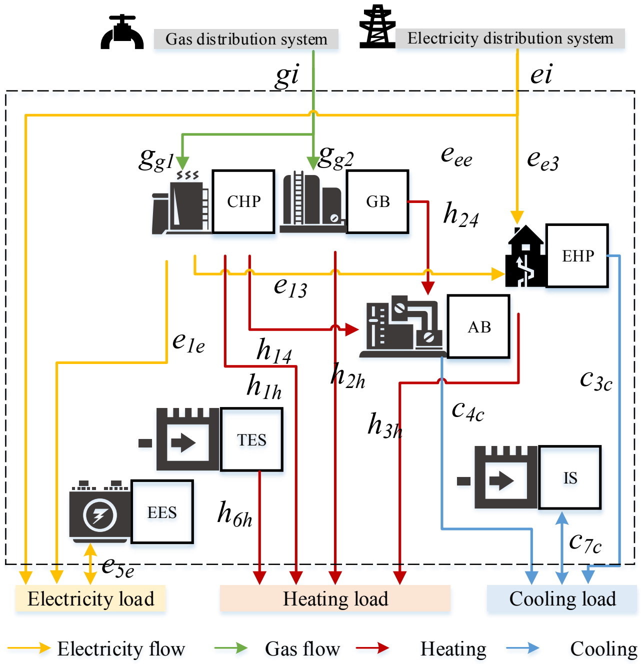

Fig. 1. Structure of the studied DMES

The structure of the studied DMES is presented in Fig. 1. The EH is responsible for converting the electricity and gas from the distribution networks into energies of electricity, heating, and cooling, respectively, to satisfy the demand of end-users. The devices in the EH include CHP, GB, EHP, AB, EES, thermal energy storage (TES), ice storage (IS), respectively. they are abstracted as different nodes.

III. Operational Reliability of DMES Components

According to different numbers of performance indicators they have, the components in the EH can be divided into two categories: single performance and multi-performance components. This difference is unique in the multi-energy systems, compared with traditional electricity systems. For example, the performance of GB is only measured by its ability to generate thermal power. On the other hand, the performance of the CHP unit is measured by both its ability to generate electricity and produce thermal power. Therefore, GB is the single performance component, and CHP is the multi-performance component. Their operational reliability models are different.

A. *Operational Reliability Model of the CHP Unit*

The CHP is a complex system that is composed of three subsystems. Their interconnections are presented in Fig. 2 [12]. The function of the prime subsystem includes fuel delivery and turbine which converts the gas to the original heat steam. Part of the heat steam goes into the electricity-generation subsystem. Some of the thermal energy goes into the heat-production subsystem and uses heat exchangers to produce hot waters, which are further delivered through the district heat networks to the end-users.

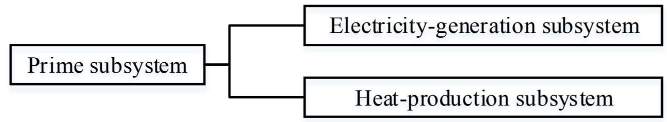

Fig. 2. Structure of the CHP system

The reliability of the three subsystems can be represented as binary state models, including the normal state and failure state. Then, the operating state of the CHP system can be calculated as:

$$s^{CHP,h} = s^p s^h, s^{CHP,e} = s^p s^e \tag{1}$$

where $s^{CHP,h}$ and $s^{CHP,e}$ are binary variables representing the state of the thermal production and electricity generation functions of the CHP unit, respectively. 1 represents the perfect functioning state, and 0 represents the failure state. s^p, s^e, and s^h are the states of prime, electricity-generation, and heat production subsystems, respectively.

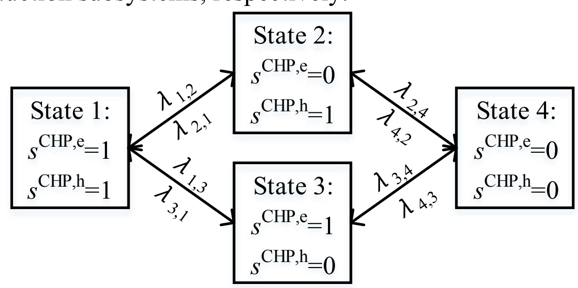

Fig. 3. State-space diagram of the CHP system

The state transitions during the operation are modeled using the Markov model[13]. The state-space diagram is presented in Fig. 3 [12]. Then, the state transition rate between any two states can be calculated as:

$$\lambda_{1,2} = \lambda^e, \lambda_{2,1} = \mu^e \tag{2}$$

$$\lambda_{1,3} = \lambda^h, \lambda_{3,1} = \mu^h \tag{3}$$

$$\lambda_{2,4} = \lambda^h + \lambda^p, \lambda_{3,4} = \lambda^e + \lambda^p \tag{4}$$

$$\lambda_{4,2} = \begin{pmatrix} \Pr\{s^p = 1, s^e = 0, s^h = 0\}\mu^h \\ + \Pr\{s^p = 0, s^e = 0, s^h = 1\}\mu^p \end{pmatrix} \Big/ \begin{pmatrix} \Pr\{s^p = 1, s^e = 0, s^h = 0\} \\ + \Pr\{s^p = 0, s^e = 0, s^h = 1\} \end{pmatrix} \tag{5}$$

$$\lambda_{4,3} = \begin{pmatrix} \Pr\{s^p = 1, s^e = 0, s^h = 0\}\mu^e \\ + \Pr\{s^p = 0, s^e = 1, s^h = 0\}\mu^p \end{pmatrix} \Big/ \begin{pmatrix} \Pr\{s^p = 1, s^e = 0, s^h = 0\} \\ + \Pr\{s^p = 0, s^e = 1, s^h = 0\} \end{pmatrix} \tag{6}$$

where $\lambda_{i,j}^{CHP}$ is the state transition rate of CHP system between state i and j . λ^e and μ^e are the failure and repair rates of the electricity-generation subsystem, which is identical for the other two subsystems. $\Pr\{\}$ represents the probability.

In the normal operating state, the feasible operating region regarding the electricity generation and thermal production of CHP is defined by a quadrangle [14]:

$$h_{1h} + h_{14} \geq 0 \tag{7}$$

$$e_{13} + e_{1e} - E_A - \frac{E_A - E_B}{(H_A - H_B)(h_{1h} + h_{14})} \leq 0 \tag{8}$$

$$e_{13} + e_{1e} - E_B - \frac{E_B - E_C}{(H_B - H_C)(h_{1h} + h_{14} - H_B)} \geq 0 \tag{9}$$

$$e_{13} + e_{1e} - E_D - \frac{E_C - E_D}{(H_C - H_D)(h_{1h} + h_{14})} \geq 0 \tag{10}$$

where (H_A, E_A), (H_B, E_B), (H_C, E_C), (H_D, E_D) are four combinations of heat and electric output of CHP, which serves as four extreme points to define a convex feasible operating region [14].

If any of the subsystems fails, the feasible operating region is derated into a projection of the original feasible region on the corresponding axis. Therefore, the new feasible region can be expressed as:

When $s^{CHP,h} = 1, s^{CHP,e} = 0$,

$$e_{13} + e_{1e} = 0 \tag{11}$$

$$\begin{aligned} &\min\{H_A, H_B, H_C, H_D\} \leq h_{1h} + h_{14} \\ &\leq \max\{H_A, H_B, H_C, H_D\} \end{aligned} \tag{12}$$

When $s^{CHP,h} = 0, s^{CHP,e} = 1$

$$h_{1h} + h_{14} = 0 \tag{13}$$

$$\begin{aligned} &\min\{E_A, E_B, E_C, E_D\} \leq e_{13} + e_{1e} \\ &\leq \max\{E_A, E_B, E_C, E_D\} \end{aligned} \tag{14}$$

When $s^{CHP,h} = 0, s^{CHP,e} = 0$, subject to (11) and (13).

B. Operational Reliability Models of Other Components

For other components with single performances, they are usually configured with redundancy and in parallel. Then, if one fails, others may cover part of the demand. Therefore, the reliability of other components can be represented using multi-state models. Take the GBs for example, the state space diagram is presented in Fig. 4. When some of the GB fails, the entire GB system will not fail completely. Instead, it will be transferred into a derated state.

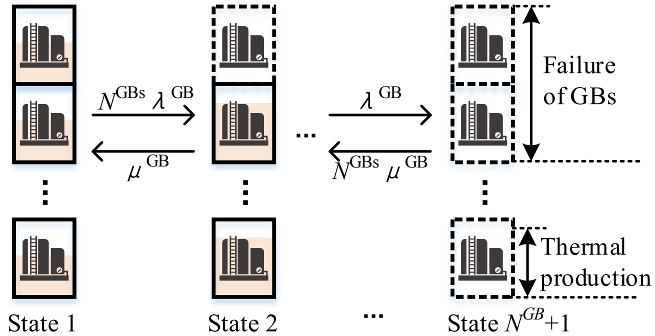

Fig. 4. State-space diagram of GBs

Suppose there are N^{GBs} GBs configured in parallel in this DMES. Then, there will be $N^{GBs}+1$ states in total. Assumes they are sorted in an ascendant order according to the available thermal production capacity. Then, the operating condition of the GBs in state s^{GB} should be limited within its capacity:

$$0 \leq h_{24} + h_{2h} \leq \frac{N^{GBs} + 1 - s^{GBs}}{N^{GBs}} ho_2^+ \tag{15}$$

where ho_2^+ is the original capacity of GBs in the perfect functioning state.

Assume only one state transition could happen at a time. Thus, the state transition could only happen between two adjacent states. The state transition rate between any two adjacent states, $\lambda_{s^{GBs},s^{GBs}+1}^{GBs}$ and $\lambda_{s^{GBs}+1,s^{GBs}}^{GBs}$ can be calculated as:

$$\lambda_{s^{GBs},s^{GBs}+1}^{GBs} = (N^{GBs} + 1 - s^{GBs})\lambda^{GB} \tag{16}$$

$$\lambda_{s^{GB}+1,s^{GB}}^{GB} = s^{GBs}\mu^{GB} \tag{17}$$

where λ^{GB} and μ^{GB} are the failure and repair rates of a single GB, respectively.

The reliability models of other components can be determined with a similar approach.

IV. OPTIMAL CONTROL OF DMES DURING COMPONENT FAILURE

Based on the operational reliability models developed in the last section, the state sequences of components during the operational horizon can be simulated using TSMCS, which is elaborated in the next section. With the given system state sequence, if there is any failed component, the optimal control should be conducted to minimize the electricity, thermal, and cooling loads, as well as minimize the energy purchasing cost of electricity and gas. Therefore, the following optimal control model is developed. The control variable $\mathbf{u}_k$ = [g_{g1}, g_{g2}, e_{ee}, e_{e3}, e_{1e}, e_{13}, h_{1h}, h_{14}, h_{2h}, h_{24}, c_{3c}, h_{3h}, c_{4c}]. $\mathbf{v}_k = [e_{5e}, h_{6h}, c_{7c}, es_5, es_6, es_7]$ are independent at each control period k . some variables are denoted in Fig. 1. Besides, es_5 , es_6 , and es_7 represent the electricity, thermal, and cooling energies stored in EES, TES, and IS, respectively.

$$Min\ \ C=\sum_{k\in K}\begin{matrix}\rho_k^g(g_{g1,k}+g_{g2,k})+\rho_k^e(e_{ee,k}+e_{e3,k})\\+\sum_{l\in\{el,th,cl\}}CDF^l(T_{s_k})lc_k^l\end{matrix} \tag{18}$$

Subject to:

1) CHP constraints:

Choose appropriate constraints from (7)-(14) according to the state of the CHP in the corresponding system state.

2) Operating constraints of GBs, EHPs, and ABs:

$$0\le c_{4c}\le co_4^+(N^{ABs}+1-s^{ABs})\ \ /N^{ABs} \tag{19}$$

$$0\le h_{3h}\le \gamma ho_3^+(N^{EHPs}+1-s^{EHPs})\ \ /N^{EHPs} \tag{20}$$

$$0\le c_{3c}\le (1-\gamma)co_3^+(N^{EHPs}+1-s^{EHPs})\ \ /N^{EHPs} \tag{21}$$

$$\mathbf{u}_k\ge 0 \tag{22}$$

3) Operating constraints for energy storages:

$$|e_{5e}|\le eo_5^+(N^{EESs}+1-s^{EESs})\ \ /N^{EESs} \tag{23}$$

$$|h_{6h}|\le ho_6^+(N^{TESs}+1-s^{TESs})\ \ /N^{TESs} \tag{24}$$

$$|c_{7c}|\le co_7^+(N^{ISs}+1-s^{ISs})\ \ /N^{ISs} \tag{25}$$

$$es_{5,k}=es_{5,k-1}+e_{5e}\Delta t \tag{26}$$

$$es_{6,k}=es_{6,k-1}+h_{6h}\Delta t \tag{27}$$

$$es_{7,k}=es_{7,k-1}+c_{7c}\Delta t \tag{28}$$

$$0\le es_{5,k}\le es_5^+(N^{EESs}+1-s^{EESs})\ \ /N^{EESs} \tag{29}$$

$$0\le es_{6,k}\le es_6^+(N^{TESs}+1-s^{TESs})\ \ /N^{TESs} \tag{30}$$

$$0\le es_{7,k}\le es_7^+(N^{ISs}+1-s^{ISs})\ \ /N^{ISs} \tag{31}$$

4) Energy conversion constraints:

$$\begin{aligned}&\mathbf{H}\begin{bmatrix}ei & gi & \mathbf{u}\end{bmatrix}^T\\&=\begin{bmatrix}d^{el}-lc^{el} & d^{th}-lc^{th} & d^{cl}-lc^{cl} & \mathbf{0}\end{bmatrix}^T\end{aligned} \tag{32}$$

where ρ^e and ρ^g are the nodal electricity and gas prices. ho_3^+, co_3^+, and co_4^+ are the heating/cooling capacities of EHP and AB. ho_3^-, co_3^-, and co_4^- are the minimum heating/cooling outputs of these devices. eo_5^+, ho_6^+, and co_7^+ are the charging and discharging power of EES, TES, and IS in the normal operating state, respectively. es_5^+, es_6^+, and es_7^+ are the capacities of these storages. γ is the operating mode of EHP. $\gamma=1$ and $\gamma=0$ represent heating and cooling modes, respectively. N^{ABs}, N^{EHPs}, N^{EESs}, N^{TESs}, and N^{ISs} are the numbers of AB, EHP, EES, TES, and IS, respectively. s^{ABs}, s^{EHPs}, s^{EESs}, s^{TESs}, and s^{ISs} are the numbers of Ass, EHPs, EESs, TESs, and ISs in the normal operating state, respectively. Δt is the time step for optimal control. *el*, *ht*, and *cl* represent the energy types of electricity, heating, and cooling, respectively.

V. Operational Reliability Evaluation Procedures

The operational reliability of DEMS is quantified using the concept of expected demand not supplied (EDNS) and loss of load probability (LOLP), which is widely adopted in the reliability evaluation in the traditional power system. in this paper, we extended these indices into a time-varying and multi-energy manner, to accommodate for the operational reliability evaluation in DMES.

$$EDNS^l(k)=\sum_{i=1}^{NS}lc_k^l\ /\ NS \tag{33}$$

$$LOLP^l(k)=\sum_{i=1}^{NS}flag(lc_k^l)\ /\ NS \tag{34}$$

Where NS is the number of simulation times. $flag(x)$ represents the flag function, where $flag(x)=1$ when $x>0$. Otherwise $flag(x)=0$.

The criterion for the convergence of TSMCS is given by the standard deviation of EDNS and LOLP:

$$\sqrt{Var(EDNS^l(k))}\ /\ EDNS^l(k)\le\xi \tag{35}$$

The whole reliability evaluation procedure can be summarized as follows:

Step 1: input data. Including the physical characteristics of the DMES, the reliability parameters, and the load profile. Set the duration of the operation horizon.

Step 2: simulate the state sequence of each component using TSMCS according to Section 3. the operational reliability models. Combine them into the system state sequence.

Step 3: formulate the optimal control problem over the operational horizon according to Section 4. Solve the linear optimal control problem using the Gurobi solver, and obtain the load curtailment for each energy.

Step 4: Calculate the reliability indices according to (33) and (34). Check (35) for convergence. If (35) satisfies, then output the operational reliability indices. Otherwise, repeat from step 2 for the next simulation.

VI. Case Studies

In this section, a test DMES is studied to validate the proposed operational reliability evaluation method. The configuration of the DMES is the same as illustrated in Fig. 1. The load curves of electricity, thermal, and cooling demands, the energy conversion efficiencies, and the capacities of the devices in the DMES are set according to [15]. The proportions of the curtailable multi-energy demand are set according to [16].

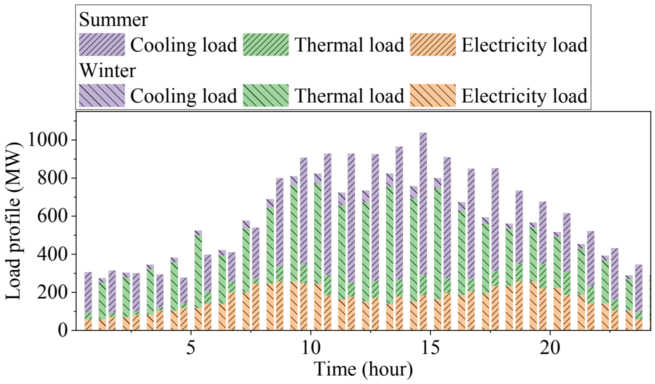

Fig. 5. Load profiles

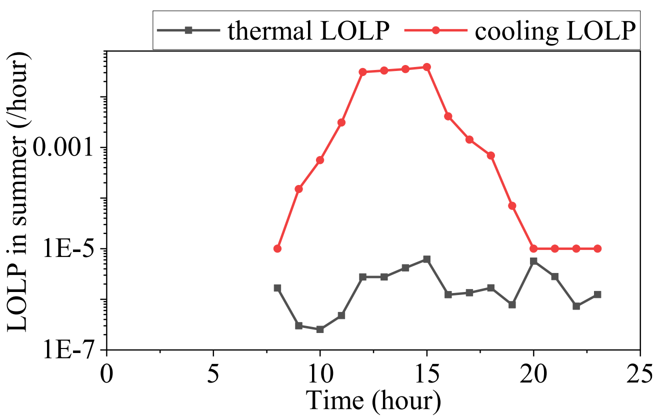

Fig. 6. LOLP in summer

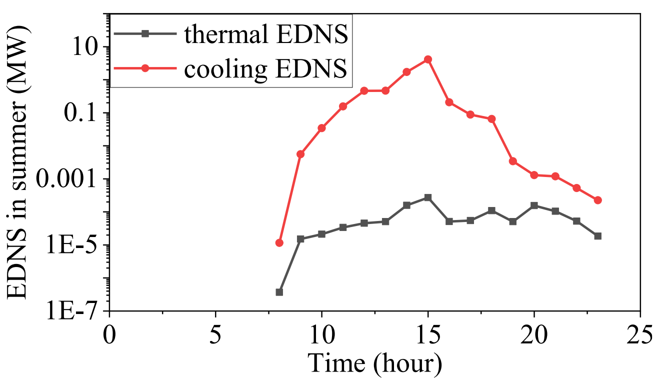

Fig.7. EDNS in summer

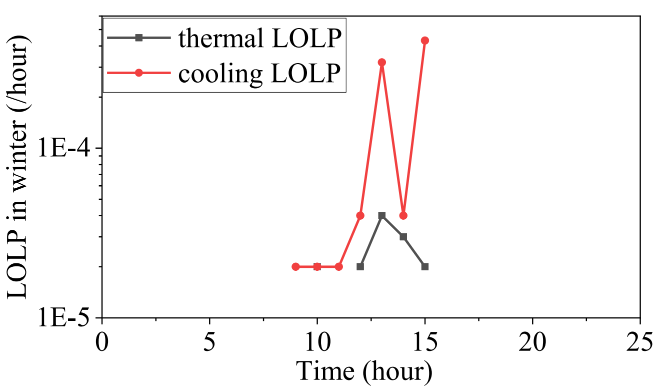

Fig. 8. LOLP in winter

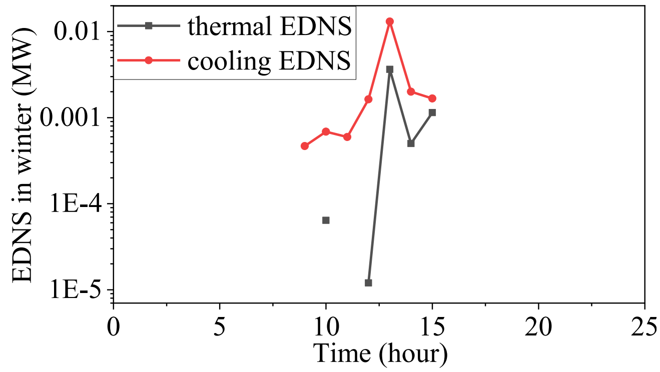

Fig. 9. EDNS in winter

The operational reliability results in summer and winter for each type of energy are presented in Fig. 5 and Fig. 6, respectively. As we can see, in any season, due to the direct interconnection with the distribution network, and we do not consider the failure of the distribution network, the EDNS, and LOLP of electricity remains zero during all the operation time. For the other two energies, generally, they remain zero until 8：00. The EDNS and LOLP emerge during 8:00-23:00. During 12:00-14:00, they reach their peak values.

In summer, due to the higher cooling load, the EHP operates in the cooling mode. If EHP fails, the cooling supply will drop instantly. Thus, the LOLP and EDNS of cooling are higher than those in winter. On the contrary, the LOLP and EDNS of thermal load are lower than those in winter.

VII. Conclusion

With the integration of multiple energies in the distribution system, maintaining reliable operation is a challenging task. This paper proposes an operational reliability evaluation method for DMES considering the optimal control strategies. Firstly, the operational reliability of the components such as CHP and GB are modeled. Then, the optimal control of the DMES during the component failures is formulated to determine the minimal load curtailments for multi-energy demands. Finally, TSMCS is used for evaluating the operational reliability indices.

The case studies show that the operational reliability indices are higher during the demand peak time. In addition, the reliabilities of thermal and cooling loads present different patterns in different seasons. The operational reliability evaluation method in this paper can further assist the distribution system operator in reliability management and other relevant decision makings.

References

[1] G. Mavromatidis, K. Orehounig, L. A. Bollinger *et al.*, “Ten questions concerning modeling of distributed multi-energy systems,” *Building and Environment,* vol. 165, pp. 106372, Nov, 2019.

[2] Energinet, "Environmental Report 2017: Environmental report for Danish electricity and CHP for 2016 status year.," July, 2018. <https://en.energinet.dk/-/media/C4170984026F4BFD921F6E852446208A.pdf>.

[3] *District Energy Systems in China*, Tsinghua University, International Energy Agency, 2017.

[4] M. Geidl, G. Koeppel, P. Favre-Perrod *et al.*, “Energy hubs for the future,” *Power & Energy Magazine IEEE,* vol. 5, no. 1, pp. 24-30, Jan-Feb, 2007.

[5] G. Koeppel, and G. Andersson, "Reliability modeling of multi-carrier energy systems," *Energy,* vol. 34(3), no. 3, pp. 235-244, Mar, 2009.

[6] M.-H. Shariatkhah, M.-R. Haghifam, M. Parsa-Moghaddam *et al.*, "Modeling the reliability of multi-carrier energy systems considering dynamic behavior of thermal loads," *Energy and Buildings,* vol. 103, pp. 375-383, Sep, 2015.

[7] H. R. Massrur, T. Niknam, J. Aghaei *et al.*, "Fast Decomposed Energy Flow in Large-Scale Integrated Electricity–Gas–Heat Energy Systems," *IEEE Transactions on Sustainable Energy,* vol. 9, no. 4, pp. 1565-1577, 2018.

[8] M.-H. Shariatkhah, M.-R. Haghifam, G. Chicco *et al.*, "Adequacy modeling and evaluation of multi-carrier energy systems to supply energy services from different infrastructures," *Energy,* vol. 109, pp. 1095-1106, Aug, 2016.

[9] M. Moeini-Aghtaie, H. Farzin, M. Fotuhi-Firuzabad *et al.*, "Generalized Analytical Approach to Assess Reliability of Renewable-Based Energy Hubs," *IEEE Transactions on Power Systems,* vol. 32(1), no. 1, pp. 368-377, Apr, 2017.

[10] Y. K. Lei, K. Hou, Y. Wang *et al.*, "A new reliability assessment approach for integrated energy systems: Using hierarchical decoupling optimization framework and impact-increment based state enumeration method," *Applied Energy,* vol. 210, pp. 1237-1250, Jan, 2018.

[11] G. Li, Z. Bie, Y. Kou *et al.*, "Reliability evaluation of integrated energy systems based on smart agent communication," *Applied Energy,* vol. 167, pp. 397-406, Apr, 2016.

[12] M. R. Haghifam, and M. Manbachi, "Reliability and availability modelling of combined heat and power (CHP) systems," *International Journal of Electrical Power & Energy Systems,* vol. 33, no. 3, pp. 385-393, Mar, 2011.

[13] J. M. Nahman, "Approximate Expressions for Steady-State Reliability Indexes of Markov Systems," *IEEE Transactions on Reliability,* vol. 35(3), no. 3, pp. 338-343, Aug, 1986.

[14] I. G. Moghaddam, M. Saniei, and E. Mashhour, "A comprehensive model for self-scheduling an energy hub to supply cooling, heating and electrical demands of a building," *Energy,* vol. 94, pp. 157-170, Jan, 2016.

[15] Y. Li, Z. Li, F. Wen *et al.*, "Privacy-Preserving Optimal Dispatch for an Integrated Power Distribution and Natural Gas System in Networked Energy Hubs," *IEEE Transactions on Sustainable Energy,* vol. 10, no. 4, pp. 2028-2038, 2019.

[16] S. Wang, C. Shao, Y. Ding *et al.*, "Operational reliability of multi-energy customers considering service-based self-scheduling," *Applied Energy,* vol. 254, pp. 113531, Nov, 2019.